Published May 16, 2011

A dynamic T cell–limited checkpoint regulates affinity-dependent B cell entry into the germinal center

Tanja A. Schwickert,[1] Gabriel D. Victora,[1,3] David R. Fooksman,[3] Alice O. Kamphorst,[1] Monica R. Mugnier,[1] Alexander D. Gitlin,[1] Michael L. Dustin,[3] and Michel C. Nussenzweig[1,2]

[1]Laboratory of Molecular Immunology and [2]Howard Hughes Medical Institute, The Rockefeller University, New York, NY 10065
[3]Helen L. and Martin S. Kimmel Center for Biology and Medicine, Skirball Institute of Biomolecular Medicine, New York University School of Medicine, New York, NY 10016

The germinal center (GC) reaction is essential for the generation of the somatically hypermutated, high-affinity antibodies that mediate adaptive immunity. Entry into the GC is limited to a small number of B cell clones; however, the process by which this limited number of clones is selected is unclear. In this study, we demonstrate that low-affinity B cells intrinsically capable of seeding a GC reaction fail to expand and become activated in the presence of higher-affinity B cells even before GC coalescence. Live multiphoton imaging shows that selection is based on the amount of peptide–major histocompatibility complex (pMHC) presented to cognate T cells within clusters of responding B and T cells at the T–B border. We propose a model in which T cell help is restricted to the B cells with the highest amounts of pMHC, thus allowing for a dynamic affinity threshold to be imposed on antigen-binding B cells.

CORRESPONDENCE
Michel C. Nussenzweig:
nussen@rockefeller.edu

Abbreviations used: AID, activation-induced cytidine deaminase; GC, germinal center; NP, 4-hydroxy-3-nitrophenylacetyl; pMHC, peptide-MHC; SA, streptavidin.

Germinal centers (GCs) are microanatomically defined structures that arise in lymphoid tissues during the immune response (MacLennan, 1994; Rajewsky, 1996). They are composed of B cells undergoing rapid clonal expansion and selection, cognate follicular helper T cells, follicular dendritic cells that capture and retain antigen on their surface, and a small number of conventional dendritic cells (MacLennan, 1994; Rajewsky, 1996; Lindquist et al., 2004; King et al., 2008). The GC reaction is of significant interest because it is the primary source of the somatically hypermutated, high-affinity antibodies that underlie immunity and autoimmunity. Most studies of how high-affinity antibodies are formed focus exclusively on the GC reaction because of its distinct anatomical, cellular, and molecular features. However, between the first contact with foreign antigen and the establishment of the GC, activated B cells progress through a series of distinct steps (Pereira et al., 2010), all or any of which could potentially impact affinity-based selection.

B cells come into contact with soluble antigen directly in B cell follicles (Pape et al., 2007). In addition, B cells can also acquire antigen bound to other lymph node–resident cell types, such as subcapsular macrophages (Carrasco and Batista, 2007; Junt et al., 2007; Phan et al., 2007), follicular dendritic cells (Suzuki et al., 2009), and lymphoid dendritic cells, both in the periphery of high-endothelial venules (Qi et al., 2006) and in the lymph node medulla (Gonzalez et al., 2010). After the initial contact with antigen, B cells travel to the border between the T cell zone and B cell follicle (T–B border) where they interact with cognate T cells to form antigen-specific cell clusters (Liu et al., 1991; Garside et al., 1998; Reif et al., 2002; Okada et al., 2005). After leaving T–B border clusters, B cells concentrate in the outer follicle in lymph nodes or in the area adjacent to the marginal zone in the spleen (Coffey et al., 2009; Pereira et al., 2010), where they proliferate for a brief period before entering the GC

T.A. Schwickert and G.D. Victora contributed equally to this paper.

The Rockefeller University Press $30.00
J. Exp. Med. Vol. 208 No. 6 1243-1252
www.jem.org/cgi/doi/10.1084/jem.20102477

Supplemental Material can be found at:
http://jem.rupress.org/content/suppl/2011/05/16/jem.20102477.DC1.html

Published May 16, 2011

reaction or developing into short-lived plasmablasts. Although the precise nature of the signals that govern this key cell fate decision is not entirely understood, high-affinity BCR cross-linking is thought to favor the plasmablast response (Paus et al., 2006). However, B cell autonomous signals alone may not be sufficient to determine B cell fate decision. In particular, cognate B and T cells in T–B border clusters engage in long-lived, dynamic contacts (Okada et al., 2005; Qi et al., 2008), which could also help direct B cells to either the GC or early antibody-forming cell fates.

Whereas GC competition and affinity maturation have been studied extensively, less is known about how antibody affinity impacts the initial selection of B cells into the GC. In this study, we make use of multiphoton intravital imaging to examine the initial events that mediate B cell selection into the GC reaction. We find that antibody affinity regulates pre-GC competition and that this process is mediated by B cell presentation of cognate antigen to T cells.

RESULTS

GC seeding is dependent on interclonal competition

To examine the role of affinity in B cell selection into the GC reaction, we made use of two strains of knockin mice carrying *Ig* heavy chains that, when combined with an Igλ light chain, produce antibodies with different affinities for the hapten 4-hydroxy-3-nitrophenylacetyl (NP; Shih et al., 2002b). High-affinity B1-8^{hi} B cells have a 40-fold higher affinity (Ka 5 × 106 M$^{1\ 1}$; K_d 2 × 10^{-7} M) for NP than low-affinity B1-8^{lo} B cells (K_a 1.25 × 10^5 M^{-1}; K_d 8 × 10^{-6} M), and WT B cells bearing native B1-8 (VH186.2, DFL16.1, and JH2) antibody genes are of intermediate affinity (K_a 5 × 10^5 M^{-1}; K_d 2 × 10^{-6} M; Allen et al., 1988).

B1-8^{hi} and B1-8^{lo} cells produce comparable NP-specific GCs in response to antigen when in a noncompetitive environment (Shih et al., 2002a). B1-8^{hi} cells also predominate in the GC when transferred into the competitive environment of a WT recipient (Schwickert et al., 2007, 2009). In contrast to high-affinity B cells, low-affinity B1-8^{lo} cells transferred into WT recipients were unable to compete with endogenous polyclonal B cells and accounted for only a fraction of total GC cells (Fig. 1, A–C). Thus, the relative affinity of the BCR determines whether a B cell will dominate the GC reaction.

To further investigate the nature of the competition, we transferred B1-8^{lo} B cells alone or in combination with competing B1-8^{hi} B cells into hosts with a limited BCR repertoire (MD4 mice; Fig. 1 A). MD4 recipients are transgenic for an Ig that is specific for hen egg lysozyme, and ∼99% of B cells in these mice express the transgenic BCR (Goodnow et al., 1988). Thus, although MD4 recipients are B cell sufficient, there are very few if any endogenous NP-specific B cells that might compete with transferred B1-8^{hi} or B1-8^{lo} cells for NP binding (Fig. S1). OT-II T cells were cotransferred with B cells to normalize T cell help between WT and transgenic hosts. As expected, transfer into this noncompetitive environment rescued the ability of B1-8^{lo} cells to dominate the GC reaction (Fig. 1, B and C). In contrast, when B1-8^{lo} cells were cotransferred into MD4 mice with B1-8^{hi}, GCs were composed almost entirely of B1-8^{hi} cells (Fig. 1 B). Quantitative analysis by flow cytometry showed a dramatic decrease in the proportion of B1-8^{lo} B cells in GCs, from 89 to 1%, in the presence of B1-8^{hi} B cells (Fig. 1 C). We conclude that a B cell clone's ability to emerge in the GC is restrained by interclonal competition.

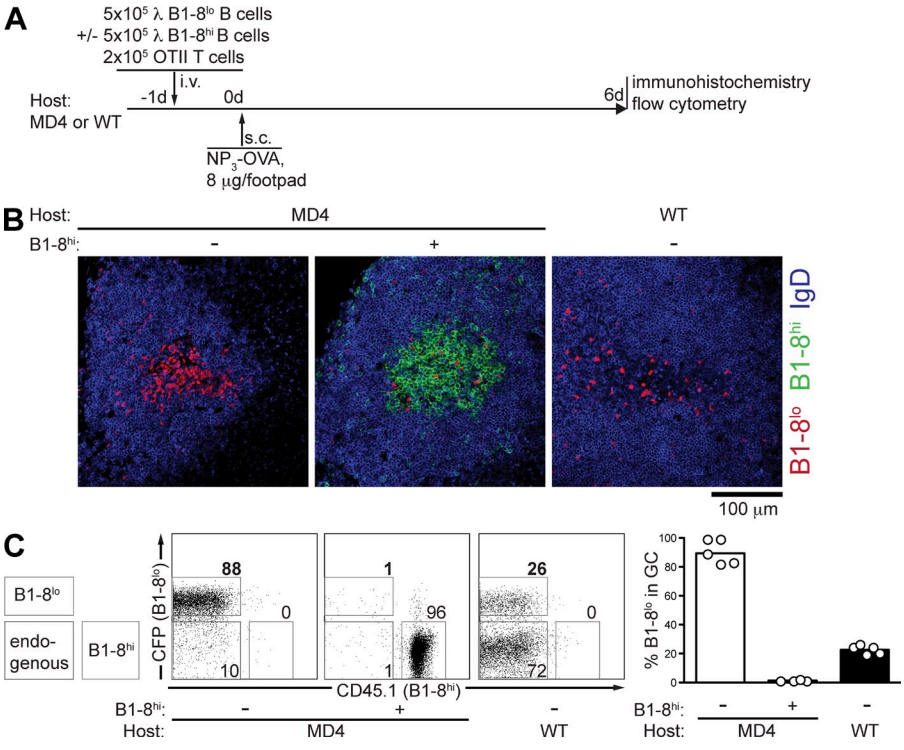

Figure 1. GC occupancy is regulated by competition. (A) Diagrammatic representation of the experimental protocol. (B) Histology showing composition of GCs in draining lymph nodes 6 d after immunization. B1-8^{lo} B cells are GFP$^+$ (false-colored red), and B1-8^{hi} B cells are CD45.1$^+$ (green). GCs were identified by absence of IgD$^+$ B cells (blue) within the B cell follicle. Images are representative of multiple GCs from two independent experiments. (C) Composition of GCs by flow cytometry. Gated on CD19$^+$Igλ$^+$FAS$^+$GL-7$^+$. (left) Representative flow cytometry plots showing the fraction of cells of each genotype (B1-8^{lo} B cells are CFP$^+$, B1-8^{hi} B cells are CD45.1$^+$, and endogenous B cells are CFP$^-$CD45.1$^-$). (right) Quantification of GC occupancy under different conditions. Each symbol represents one mouse. Data are from two independent experiments with two to three mice per condition per experiment.

Published May 16, 2011

Competition inhibits B cell proliferation and activation before GC coalescence

B1-8^{hi} cells dominate GCs as early as day 6 after immunization, even in the presence of large numbers of B1-8^{lo} naive precursors, suggesting that competitive selection might occur even before GCs are fully established. To investigate this possibility, we examined B cells responding to NP on day 4 after immunization (Fig. 2), before GCs can be detected by histology or flow cytometry (Fig. S2). On day 4 after independent transfer into MD4 mice and challenge with cognate antigen, both B1-8^{hi} and B1-8^{lo} B cells divided extensively and began to up-regulate activation markers, some of which are associated with the GC (FAS and GL-7 antigen; Fig. 2 and Fig. S2). However, these early responding B cells were phenotypically distinct from authentic GC cells because they remained IgD^{+} and expressed high levels of the chemokine receptor CCR6 (Fig. S2). Thus, FAS^{int}GL-7^{+}IgD^{+}CCR6^{hi} B cells represent a transitional stage between naive and GC B cell phenotypes (pre-GC B cells).

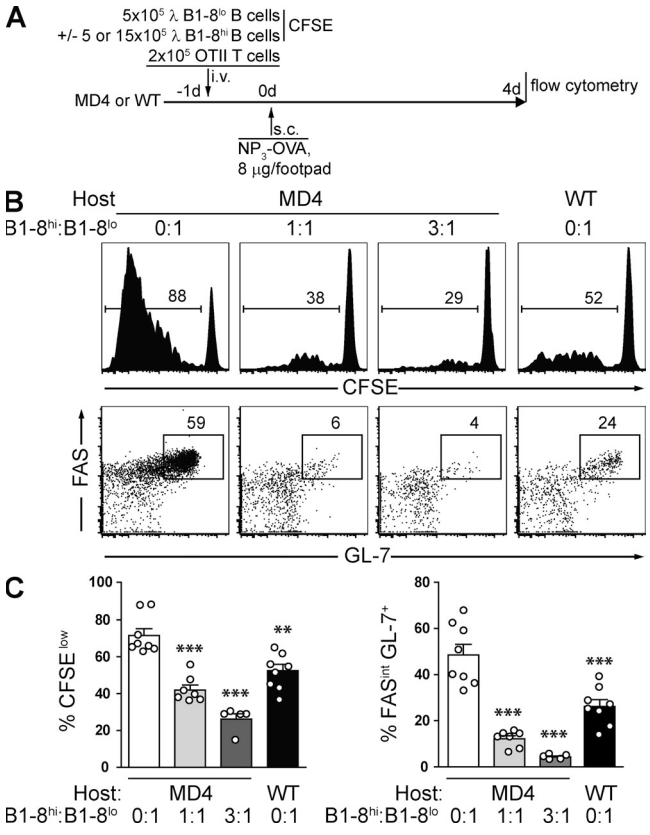

Figure 2. Competition inhibits early proliferation and activation of low-affinity B cells. (A) Diagrammatic representation of the experimental protocol. (B) Flow cytometric analysis of transferred B1-8^{lo} CD45.1^{+} CFSE-labeled B cells in draining lymph nodes 4 d after immunization. Gated on CD19^{+}Igλ^{+}CD45.1^{+} cells. (top) Representative CFSE dilution histograms. (bottom) Representative FAS/GL-7 dot plots. (C) Quantification of B. (left) Percentage of divided (CFSE^{low}) B1-8^{lo} B cells. (right) Percentage of FAS^{int}GL-7^{+} B1-8^{lo} cells. Each symbol represents one mouse. Error bars are SEM. Data are from three independent experiments with one to three mice per condition per experiment. **, $P < 0.01$; ***, $P < 0.001$ compared with B1-8^{lo} in MD4 host.

To determine whether affinity-dependent competition occurs before GC formation, we transferred B1-8^{lo} B cells with or without B1-8^{hi} into MD4 or WT hosts and measured proliferation by CFSE dilution on day 4 after immunization (Fig. 2 A). Although proliferation was readily detected when B1-8^{lo} cells were transferred alone (mean 72% CFSE^{low}), cotransfer of B1-8^{hi} cells at a 1:1 ratio inhibited B1-8^{lo} proliferation (mean 42% CFSE^{low}). Cotransfer of a threefold excess of B1-8^{hi} B cells caused a further drop in CFSE^{low} cells to 26% (Fig. 2, B and C). Similarly, the proportion of pre-GC B1-8^{lo} B cells decreased from 61% when B1-8^{lo} were transferred alone to 15% and 4% when cotransferred with B1-8^{hi} at 1:1 and 1:3 ratios, respectively (Fig. 2, B and C). Competition between B1-8^{lo} B cells and the endogenous NP-specific repertoire in WT recipients resulted in an intermediate degree of inhibition of proliferation and activation compared with transfer into MD4 mice (Fig. 2, B and C). We conclude that affinity-based competition between B cells occurs before GCs are established and that NP-specific precursor frequency is an important factor in determining the outcome of competition.

Antigen binding and presentation are not inhibited by competition

The affinity-based inhibition of proliferation and activation detected early in GC B cell differentiation implies that antigen-specific B cells are competing for access to a limiting factor. A potential factor limiting this differentiation could be antigen availability. To determine whether the presence of competing B cells alters the amount of antigen bound or presented by B1-8^{lo} B cells, we generated a chimeric antigen consisting of streptavidin (SA) covalently coupled to both NP and Alexa Fluor 647 (a pH-insensitive fluorophore) and bound to biotinylated I-Eα$_{52–73}$ peptide (NP-Eα; Fig. S3 A). This reagent allows for the quantification of both the amount of antigen bound by a B cell (by direct measurement of cell-associated Alexa Fluor 647 fluorescence) and of MHC class II presentation (by staining with peptide-MHC [pMHC]–specific antibody Y-Ae; Fig. S3 B; Rudensky et al., 1991). To measure the influence of competition on antigen capture, we transferred B1-8^{lo} cells into MD4 hosts in the presence or absence of B1-8^{hi} B cells or into WT hosts and immunized recipients with NP-Eα in alum. B cell–associated antigen and antigen presentation on MHC II were measured 16 h later by flow cytometry (Fig. 3 A). A similar proportion of B1-8^{lo} B cells (~50%) bound and presented similar amounts of antigen, regardless of the presence or absence of B1-8^{hi} B cells or of recipient host (WT vs. MD4; Fig. 3, B and C). Thus, the amount of antigen captured and presented by low-affinity B cells is not altered by competition with high-affinity cells but instead shows a remarkable correlation with BCR affinity. B1-8^{hi} cells, whose BCRs have a 40-fold higher affinity to NP than those of B1-8^{lo} cells, show a two- to threefold higher level of antigen uptake and a three- to fourfold higher level of pMHC presentation when compared with their lower-affinity

Published May 16, 2011

counterparts (Fig. 3, B and C). Most importantly, even though their proliferation at later time points is severely impaired, B1-8^{lo} B cells capture, process, and present on MHC II the same amount of antigen, irrespective of the presence of competing B cells. We conclude that, under the conditions tested, competition for antigen acquisition or for BCR-delivered signals does not play a limiting role in pre-GC expansion.

Additionally, we tested whether antigen dose is limiting for B cell proliferation and activation by conducting antigen titration experiments in MD4 mice receiving B1-8^{lo} cells or 1:1 mixtures of B1-8^{lo} and B1-8^{hi} B cells. Mice were immunized with 5, 50, or 200 µg of antigen, and B cell activation and proliferation were measured by flow cytometry (Fig. 4 A). Surprisingly, proliferation and activation of B1-8^{lo} B cells was always decreased to approximately half in the presence of cotransferred B1-8^{hi} B cells, regardless of antigen dose (Fig. 4, B and C). Thus, although the extent of cell division and activation is dependent on the concentration of antigen, competition between antigen-specific B cells is not, and affinity-dependent competition between pre-GC B cells is detectable over a wide range of antigen doses.

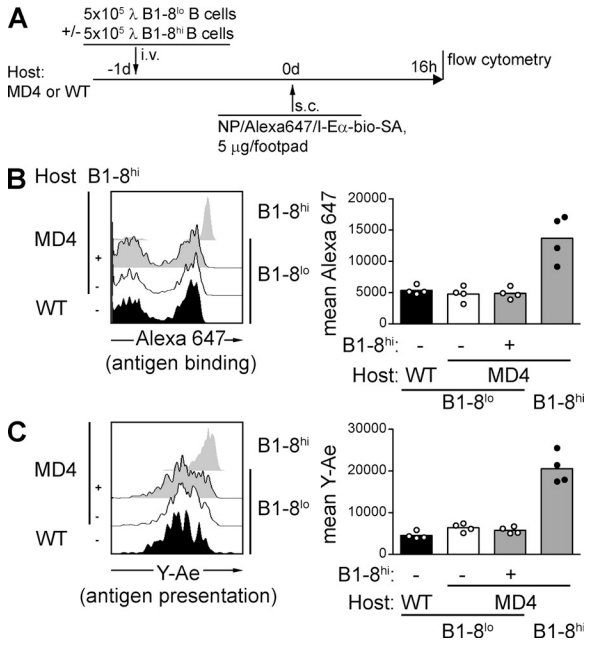

Figure 3. Competition does not affect antigen binding and presentation by low-affinity B cells. (A) Diagrammatic representation of the experimental protocol. (B, left) Flow cytometric analysis of antigen binding by B1-8^{hi} and B1-8^{lo} cells under different transfer conditions. Gated as CD19$^+$Igλ^+CD45.1$^+$ (B1-8^{hi}) or CD19$^+$Igλ^+CFP$^+$ (B1-8^{lo}). (right) Quantification of flow cytometry data. (C, left) Flow cytometric analysis of antigen presentation by B1-8^{hi} and B1-8^{lo} cells under different transfer conditions. Cell types are gated as in B; only Alexa Fluor 647$^+$ cells are plotted. The Y-Ae antibody binds to the I-Eα_{52-68} peptide in the context of I-A^b. (right) Quantification of flow cytometry data. Each symbol represents one mouse. Data are from two independent experiments with two mice per condition per experiment.

Increased access to T cell help provides a competitive advantage to pre-GC B cells

Even if access to, uptake, and presentation of antigen remain unaltered by competition, the observed inhibition of B1-8^{lo} cell activation and proliferation could still be mediated by the availability of T cell help. In this model, a limiting number of helper T cells would interact preferentially with pre-GC B cells presenting the highest density of cognate pMHC at the T–B border stage, as was shown to occur in the GC (Victora et al., 2010). To test this idea, we first examined the effect on pre-GC competition of increasing the amount of antigen-specific T cells. To this end, we transferred an equal number of B1-8^{lo} and B1-8^{hi} Igλ^+ B cells along with either 2×10^5 or 2×10^6 OT-II T cells and measured B cell proliferation and activation at day 4 after immunization (Fig. S4). Increasing the number of antigen-specific T cells led to an overall increase in both B1-8^{hi} and B1-8^{lo} proliferation and activation, indicating that T cell help is indeed limiting at this early stage.

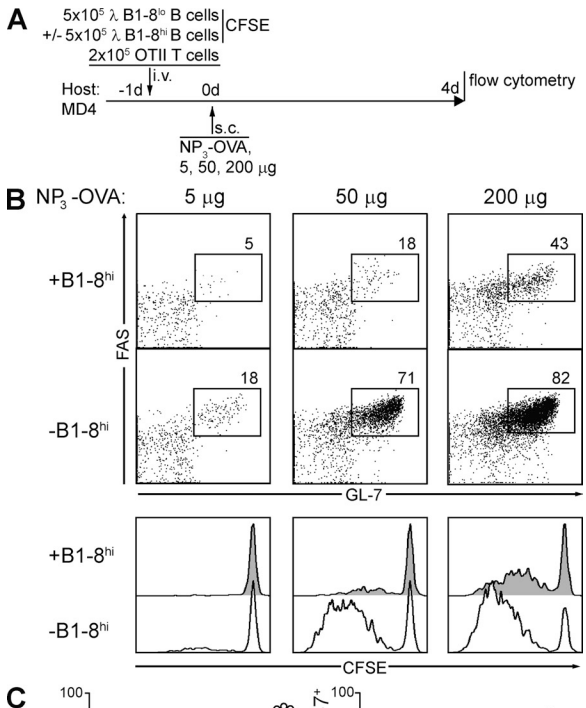

Figure 4. Inhibition of proliferation/activation by competition is independent of antigen dose. (A) Diagrammatic representation of the experimental protocol. (B) Flow cytometric analysis of transferred B1-8^{lo} CD45.1$^+$ CFSE-labeled B cells in draining lymph nodes 4 d after immunization. Gated on CD19$^+$Igλ^+CD45.1$^+$. (top) Representative FAS/GL-7 plots. (bottom) Representative CFSE histogram. (C) Quantification of data in B. Each symbol represents one mouse. Data are from two independent experiments with two to three mice per condition per experiment.

Published May 16, 2011

Furthermore, there was a slight decrease in the effect of B1-8^{hi} competition on B1-8^{lo} proliferation/activation, suggesting that the availability of T cell help could also play a role in pre-GC competition.

To test this hypothesis under more controlled conditions, we delivered antigen to B cells without cross-linking surface Ig by targeting it directly to cells that express DEC205 using a chimeric anti-DEC205 antibody fused to OVA (α-DEC205–OVA; Bonifaz et al., 2002). Activated B cells expressed low levels of DEC205, a cell surface lectin that efficiently delivers antigen to the MHC II processing compartment (Fig. S5 A; Jiang et al., 1995; Kamphorst et al., 2010). Chimeric antibodies to this receptor, linked to protein antigens such as OVA, target these antigens to DEC205-expressing APCs, including B cells and dendritic cells. To examine the impact of increased pMHC on proliferation and activation, we cotransferred allotype-marked B1-8^{hi} B cells that were either DEC205 deficient or sufficient (DEC205$^{-/-}$ or DEC205$^{+/+}$), along with OVA-specific OT-II T cells, into DEC205$^{-/-}$ hosts. Recipient mice were then immunized with NP-OVA and treated with α-DEC205–OVA, PBS, or a control chimeric DEC205 antibody carrying an irrelevant antigen, *Plasmodium falciparum* circumsporozoite protein (α-DEC205–CS; Boscardin et al., 2006), to exclude an effect of DEC205 receptor ligation on B cell activation (Fig. 5 A). DEC205$^{+/+}$ and DEC205$^{-/-}$ B1-8^{hi} pre-GC B cells showed similar levels of proliferation and activation in mice treated with PBS or α-DEC205–CS. Approximately 76% of cells in both populations were CFSE^{low}, and 34% were GL-7^{+} and FAS^{+} (Fig. 5 B). In contrast, when mice received α-DEC205–OVA, the DEC205$^{+/+}$ B1-8^{hi} population outcompeted the DEC205$^{-/-}$ B1-8^{hi} B cells in terms of both proliferation and activation. Proliferation by DEC205$^{+/+}$ B cells, as measured by CFSE dilution, increased from 76 to 89%, and the percentage of activated B cells doubled to 68%. Most importantly, the DEC205$^{-/-}$ B1-8^{hi} B cells displayed a lower level of proliferation (60 vs. 76%) and activation (17 vs. 34%) when compared with mice receiving either the control antibody α-DEC205–CS or PBS, despite receiving similar amounts of NP-OVA antigen (Fig. 5 C). To test whether increasing T cell help alone could compensate for the large difference in affinity between B1-8^{hi} and B1-8^{lo} B cells, we cotransferred a 1:1 mixture of B1-8^{lo}, DEC205$^{+/+}$, and B1-8^{hi} DEC205$^{-/-}$ Igλ^{+} B cells, along with OT-II T cells, into DEC205$^{-/-}$ MD4 recipients and immunized these hosts with NP-OVA (Fig. S5, B and C). When recipients were treated with PBS or control α-DEC205–CS after immunization, B1-8^{lo} proliferation/activation was substantially lower than that of B1-8^{hi} cells. Treatment with α-DEC205–OVA was capable of restoring B1-8^{lo} proliferation/activation to near B1-8^{hi} levels in 3/5 mice (Fig. S5 C).

To determine whether the competitive advantage in proliferation and activation provided by increased T cell help is associated with increased GC occupancy, we examined the composition of GCs produced under the same conditions 6 d after immunization (Fig. 6 A). Whereas GCs in mice treated with anti-DEC205–CS or PBS were composed of nearly equal numbers of DEC205$^{+/+}$ and DEC205$^{-/-}$ B cells, treatment with anti-DEC205–OVA resulted in GCs that were almost exclusively filled with DEC205$^{+/+}$ B1-8^{hi} B cells (Fig. 6, B and C). We conclude that increasing the density of pMHC on the B cell surface is sufficient to provide a competitive advantage to pre-GC B cells in conditions of equal BCR cross-linking.

B cells with higher pMHC density monopolize T cell help in T–B border clusters

To directly test the idea that increased antigen presentation leads to enhanced T cell interaction and to verify that T cell signals are limiting during the pre-GC stage, we set out to observe the interactions between T cells and B1-8^{hi} B cells by multiphoton laser-scanning microscopy of lymph nodes in living mice. To this end, we transferred CFP-expressing DEC205$^{+/+}$, GFP-expressing DEC205$^{-/-}$ B1-8^{hi} B cells,

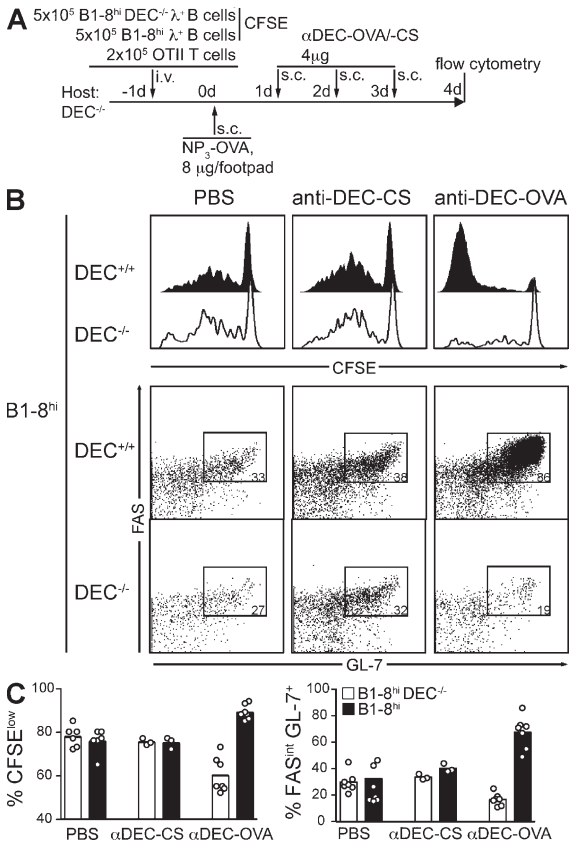

Figure 5. Access to T cell help drives early B cell competition. (A) Diagrammatic representation of the experimental protocol. (B) Flow cytometric analysis of transferred B1-8^{hi}DEC205$^{+/+}$CFP^{+} and B1-8^{hi}DEC205$^{-/-}$CD45.1^{+} CFSE-labeled B cells in draining lymph nodes 4 d after immunization. Gated on CD19^{+}Igλ^{+}CD45.1^{+} (B1-8^{hi}DEC205$^{+/+}$) or CD19^{+}Igλ^{+}CFP^{+} (B1-8^{hi}DEC205$^{+/+}$) cells. (top) Representative CFSE dilution profile. (bottom) Representative FAS/GL-7 plot. (C) Quantification of data in B. Each symbol represents one mouse. Data are from three independent experiments with one to two mice per condition per experiment. CS, *P. falciparum* circumsporozoite protein (used as a control antigen).

Published May 16, 2011

and dsRed-expressing OT-II T cells into DEC205$^{-/-}$ recipients. Mice were then immunized with NP-OVA and treated with α-DEC205–OVA or control α-DEC205–CS. In vivo imaging of the T and B cell clusters at the T–B border in popliteal lymph nodes was performed 36–48 h after immunization (Fig. 7 A). Long-lasting (>10 min) motile T–B cell interactions, indicative of active T cell help (Okada et al., 2005), were counted (Fig. 7 B and Videos 1 and 2). In control mice treated with α-DEC205–CS, we found similar frequencies of long-lasting motile conjugates between OT-II cells and B1-8^{hi} DEC205$^{+/+}$ and DEC205$^{-/-}$ B cells (Fig. 7, B and C; and Video 1). In contrast, in mice treated with α-DEC205–OVA, 90% of all specific T–B cell interactions were between OT-II T cells and DEC205$^{+/+}$ B1-8^{hi} B cells (Fig. 7 C and Video 2). We conclude that T cell signals are limiting for affinity selection of pre-GC B cells and that T cells preferentially interact with B cells with a higher density of surface pMHC.

DISCUSSION

GCs are seeded by a small number of precursor clones that expand, mutate, and undergo affinity-dependent selection (Kroese et al., 1987; Jacob et al., 1991; Liu et al., 1991). GC selection plays a major role in limiting clonal diversity and is regulated in large part by follicular helper T cells (Victora et al., 2010). Less is known about the role of affinity in the initial events that lead to GC formation. B cells are activated to enter the GC reaction by BCR cross-linking in the B cell follicle, at the lining of the subcapsulary sinus, or while migrating through the T cell area (Qi et al., 2006; Carrasco and Batista, 2007; Junt et al., 2007; Phan et al., 2007; Suzuki et al., 2009). Signals from the BCR direct activated B cells to the T–B border, where they can encounter cognate T cells (Garside et al., 1998; Okada et al., 2005). Although only B cells specific for the immunizing antigen are thought to relocate to the T–B border, B cells with very low affinity for NP, such as B1-8^{lo} B cells, with a K_a of 1.25 × 10^5 M^{-1} and K_d of 8 × 10^{-6} M, and T1(V23)μ^a cells, whose affinity is too low to reliably measure, are still capable of forming GCs (Dal Porto et al., 2002;

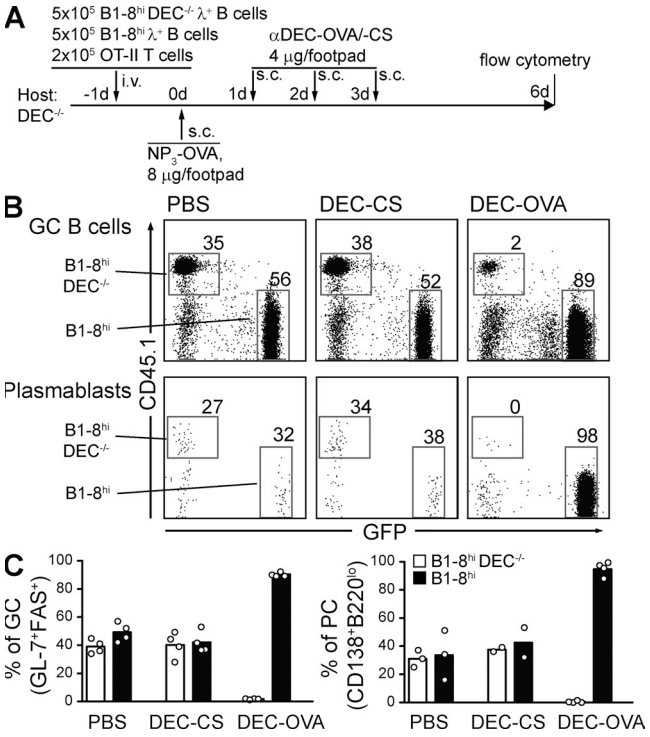

Figure 6. Increased T cell help drives greater GC occupancy and plasmablast differentiation. (A) Diagrammatic representation of the experimental protocol. (B) Flow cytometric analysis of transferred B1-8^{hi}DEC205$^{+/+}$CFP$^+$ and B1-8^{hi}DEC205$^{-/-}$CD45.1$^+$ B cells in draining lymph nodes 6 d after immunization. (top) GC occupancy. Gated on CD19$^+$Igλ$^+$GL-7$^+$FAS$^+$. (bottom) Composition of plasmablast compartment. Gated on CD138^{hi}B220^{int}. (C) Quantification of data in B. Each symbol represents one mouse. Data are from three independent experiments with one to two mice per condition per experiment. CS, *P. falciparum* circumsporozoite protein (used as a control antigen).

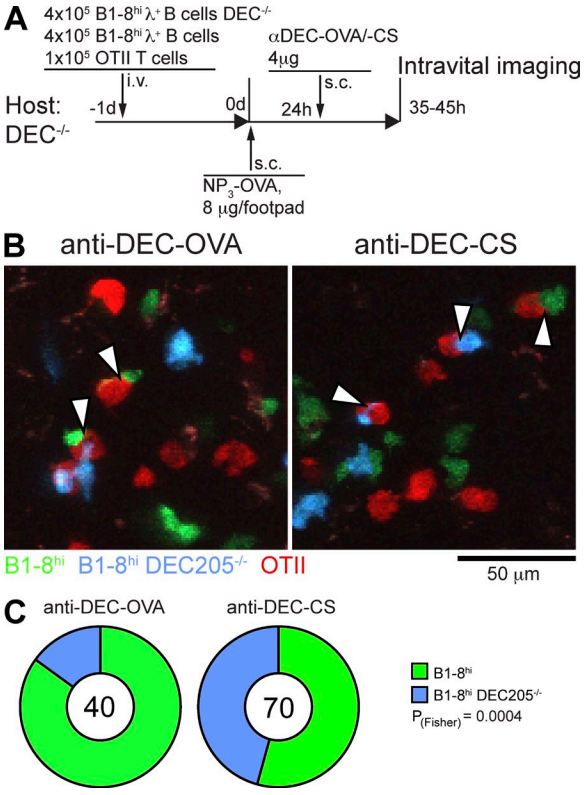

Figure 7. B cells with higher surface MHC preferentially interact with cognate T cells at the T–B border. (A) Diagrammatic representation of the experimental protocol. (B) Collapsed z stacks of three-dimensional image series of T–B border clusters in living mice. Arrowheads indicate long-lasting conjugates (>10 min) between OT-II T cells (red) and either B1-8^{hi}DEC205$^{+/+}$ (green) or B1-8^{hi}DEC205$^{-/-}$ (cyan) B cells. (C) Quantification of T–B cell interactions in intravital videos. Pie charts represent the proportion of long-lasting T–B conjugates involving DEC205$^{+/+}$ and DEC205$^{-/-}$ B1-8^{hi} B cells. The total number of conjugates analyzed is indicated in the center of each chart. The charts represent pooled data from multiple videos taken from three independent experiments, one mouse per condition per experiment. CS, *P. falciparum* circumsporozoite protein (used as a control antigen).

Published May 16, 2011

Shih et al., 2002a). In addition, the artificially reverted germline versions of naturally occurring high-affinity, somatically mutated antibodies to antigens such as HIV show very low affinities to antigen (Scheid et al., 2009; Mouquet et al., 2010). Thus, the absolute affinity threshold for the initial event that triggers the B cell GC program must be very low. In this study, we address the question of how GC founder B cells are selected from among the relatively large number of naive B cells intrinsically capable of passing this low BCR-dependent activation threshold.

We show evidence for an affinity-dependent checkpoint operating within clusters of B and T cells that form at the T–B border within 1–2 d of immunization. Our data show that competition from higher-affinity B cells impairs the ability of lower-affinity B cells to become activated, proliferate, and eventually reach an intermediary pre-GC stage characterized by up-regulation of FAS, GL-7, and CCR6. Although these findings do not argue against the existence of a threshold affinity for B cell activation, they indicate that additional layers exist that restrict the breadth of the early B cell response.

Our antigen acquisition and processing data suggest that competition does not limit access to antigen delivered subcutaneously in alum. High-affinity B cells acquire more antigen than low-affinity cells, but the presence of the former has no measurable effect on antigen acquisition by the latter. In addition, pre-GC competition is comparable across a range of different antigen concentrations, which also argues against a model in which B cells compete for relative access to antigen. However, our experiments do not rule out the possibility of competition for antigen acquisition under other conditions, such as when small amounts of antigen are delivered by direct transfer from other cells (Qi et al., 2006; Carrasco and Batista, 2007; Junt et al., 2007; Phan et al., 2007; Suzuki et al., 2009; Gonzalez et al., 2010). Thus, it remains possible that direct competition for access to antigen would provide an additional checkpoint to prevent B cells with relatively lower affinities for antigen from entering the GC.

Within GCs, B cells compete for T cell help. B cells with high-affinity BCRs residing in the light zone of the GC capture more antigen and present a higher level of cognate pMHC on their surfaces than low-affinity cells. Follicular helper T cells interact preferentially with the B cells presenting the highest levels of pMHC and induce them to move to the dark zone where they undergo proliferative expansion (Victora et al., 2010). Similarly, the absence of H2-O, an MHC family molecule that inhibits peptide presentation, confers a competitive advantage to GC B cells (Draghi and Denzin, 2010), and increased T cell help in Roquin-deficient or Qa-1(D227K) mice leads to inappropriate GC B cell activation and autoimmunity (Vinuesa et al., 2005; Kim et al., 2010). Our data show that T cell help is also essential for affinity-dependent B cell selection at the T–B border. As in the GC, T–B border T cells mediate selection by distinguishing among B cells on the basis of the amount of cognate pMHC presented. Artificially increasing pMHC on high-affinity cells through DEC205 targeting of antigen had a dramatic effect on T–B border competition, GC seeding, and plasma cell differentiation. However, the same approach was capable of rescuing the proliferation of low-affinity cells in only 3/5 recipients (Fig. S5, B and C). Although the reasons for such variability are unclear, it may indicate the existence of further checkpoints to the progression of B1-8^{lo} cells into a productive GC response, perhaps even at the level of antigen binding. However, technical issues, such as an inability to increase pMHC levels on B1-8^{lo} cells to a level higher than that presented by the DEC205$^{-/-}$ B1-8^{hi} cells, cannot be discounted.

Although B cells in pre-GC T–B border clusters can be distinguished from GC B cells by microanatomic location and cell surface markers (Fig. S2), the two cell types share certain characteristics such as brisk proliferation, activated B cell morphology, and engagement in motile contacts with helper T cells (Okada et al., 2005). One important difference between such B cells in T–B border clusters and GC cells is the duration of T–B conjugates, which are much longer-lived in T–B border clusters (Okada et al., 2005; Allen et al., 2007; Fooksman et al., 2010). These long-lived contacts provide the ideal setting for T cell–mediated selection. Our experiments show that higher-affinity B cells with higher cognate pMHC surface densities monopolize T cell help, physically interfering with a T cell's ability to interact with low-affinity B cells. The data suggest a dynamic mechanism that accounts for pre-GC competition in which BCR affinity serves as a determinant of the amount of peptide presented on the B cell surface; B cells with higher pMHC densities would compete favorably for access to helper T cells, leading to the proliferation of higher-affinity B cells and to the gradual elimination of lower-affinity cells from the reaction.

The GC reaction is critical to the production of high-affinity antibodies because it is the microanatomic location wherein B cells express activation-induced cytidine deaminase (AID; Muramatsu et al., 2000). Although AID has a strong preference for Ig genes, it also produces mutations in bystander oncogenes such as Bcl6 (Pasqualucci et al., 1998; Shen et al., 1998), and it is responsible for initiating chromosome translocations such as those between c-myc and IgH, which produce Burkitt's lymphoma and plasmacytoma (Robbiani et al., 2008, 2009). One clear advantage of an affinity-based pre-GC checkpoint is the economy of resources provided by limiting the number of B cell clones undergoing the GC reaction; an additional advantage is limiting the number of clones exposed to AID. In contrast, the ability to engage low-affinity clones and the low threshold for B cell activation in vivo is likely to be essential to ensuring that there will be an initial response to antigen, irrespective of B cell precursor frequency or initial affinity. Early competition before the GC prevents the costly expansion of a substantial number of low-affinity clones. A potential disadvantage to limiting the number of clones that participate in GC responses is the emergence of immunodominant epitopes, which may be exploited by pathogens to direct antibodies away from neutralizing epitopes. This seems to be the case with influenza, where the generation of antibodies to broadly neutralizing epitopes on the

Published May 16, 2011

hemagglutinin stem seems to be prevented by competition from more "attractive" epitopes on the protein head (Ekiert et al., 2009), and may also be the case in HIV infection (Scheid et al., 2009). Thus, the evolution of a pre-GC affinity-dependent selection checkpoint may have been shaped by the need to produce high-affinity antibodies to pathogens while preventing excessive exposure to AID-induced mutagenesis.

MATERIALS AND METHODS

Mice. C57BL/6 (WT), B6.SJL (CD45.1$^+$), and mice transgenic for GFP (Schaefer et al., 2001), CFP (Hadjantonakis et al., 2002), and dsRed (Vintersten et al., 2004) were purchased from the Jackson Laboratory. MD4 BCR-transgenic (Goodnow et al., 1988) and OT-II TCR-transgenic (Barnden et al., 1998) mice were maintained at the Rockefeller University. B1-8^{hi} and B1-8^{lo} IgH knockin (Shih et al., 2002b) and DEC205$^{-/-}$ mice (Guo et al., 2000) were generated and maintained in our laboratory. All mice were on a C57BL/6 background. For adoptive transfer experiments, donor mice were 8–16 wk and recipients were 6–10 wk of age. Mice were housed under specific pathogen-free conditions. The animal protocol was approved by the Rockefeller University.

Cell transfer, immunization, and antigens. B cells were purified by immunomagnetic depletion with anti-CD43 beads (Miltenyi Biotec). For flow cytometry experiments, 5×10^6 B1-8^{hi} total B cells (5×10^5 B1-8^{hi} NP-specific Igλ$^+$ B cells) and 15×10^6 B1-8^{lo} total B cells (5×10^5 B1-8^{lo} NP-specific Igλ$^+$ B cells) were transferred intravenously before immunization. For histology and in vivo imaging, NP-specific B cells were further enriched by depletion of Igκ$^+$ cells using anti–Igκ-PE (BD) followed by anti-PE beads (Miltenyi Biotec). For in vivo imaging, 4×10^5 Igλ$^+$ B1-8^{hi} DEC205$^{+/+}$ and 4×10^5 Igλ$^+$ B1-8^{hi} DEC205$^{-/-}$ B cells were transferred. OT-II T cells were purified by immunomagnetic depletion with a CD4$^+$ T cell isolation kit (Miltenyi Biotec). 2×10^5 OT-II T cells were cotransferred along with the B cells in all experiments involving B cell activation or proliferation. 1 d after B cell transfer, mice were immunized with NP_3-OVA precipitated in alum (2:1). Mice were injected subcutaneously with 8 μg NP_3-OVA per footpad and 16 μg into the base of the tail. For antigen pick-up and presentation experiments, mice were immunized with 5 μg NP-Eα precipitated in alum (2:1) in both hind footpads. For NP-PE binding experiments, mice were injected subcutaneously with 8 μg NP_{25}-PE (Biosearch Technologies) per footpad and 16 μg into the base of the tail. For targeting of antigens via DEC205, mice were injected subcutaneously with α-DEC205–OVA or α-DEC205–CS into each hind footpad at the dose indicated in each figure.

Production of the NP-Eα regent. NP succinimidyl ester (Biosearch Technologies) was conjugated to either purified SA (ProZyme) or SA–Alexa Fluor 647 (Invitrogen) to a hapten to protein ratio of ∼10. This conjugate was then incubated with sixfold molar excess of biotinylated $E\alpha_{52–73}$ peptide preceded by a flexible Gly-Ser-Gly linker (full sequence, biotin-GSGFAK-FASFEAQGALANIAVDKA-COOH), and free peptide was removed by dialysis. Nonhaptenylated SA and SA–Alexa Fluor 647 were also bound to biotinylated peptide as a control. For testing purposes, purified splenic B1-8^{hi} B cells were incubated in complete RPMI with 10% FCS supplemented with 1 μg/ml NP-Eα or control reagents for 18 h at 37°C and 5% CO_2. Surface pMHC expression was detected by flow cytometry using the Y-Ae antibody.

Flow cytometry. Lymph nodes were forced through a 70-μm mesh into PBS supplemented with 2% fetal calf serum and 1 mM EDTA. Single-cell suspensions were incubated for 5 min with 1 μg/ml anti-CD16/32 (24G2; eBioscience) and then stained for 30 min at 4°C using the antibodies indicated in Table S1. Samples were acquired using a flow cytometer (LSRII; BD). Data were analyzed using FlowJo version 8 software (Tree Star) for Macintosh.

Immunofluorescence. Cryostat sections of lymph nodes were fixed and stained as described previously (Lindquist et al., 2004). In brief, organs were fixed in PBS with 4% paraformaldehyde and 10% sucrose and cryoprotected in PBS with 30% sucrose before being embedded in OCT compound (Sakura) and frozen. Frozen lymph nodes were sectioned (20-μm thickness) on a microtome and fixed in acetone. For immunostaining, all incubations were performed in a humidified chamber at room temperature. Sections were blocked in 5% BSA, 10% goat serum, and sequentially with excess SA and biotin (Vector Laboratories). The following antibodies were used for staining: anti-IgD–Alexa Fluor 647 (eBioscience), anti–CD45.1-PE (BD), CD35-biotin (BD), and SA-Cy3 (Jackson ImmunoResearch Laboratories, Inc.).

Confocal microscopy. Confocal images were acquired on an LSM 510 system (Carl Zeiss) with 488-, 543-, and 633-nm excitation lines at the Rockefeller University Bio-Imaging Resource Center. Z-stack (three planes, 3-μm z steps) images were obtained with a Plan-Apochromat 20× NA 0.75 air objective. Images were acquired using LSM software (Carl Zeiss) and processed for presentation using Photoshop CS4 (Adobe).

Multiphoton laser-scanning microscopy. Multiphoton imaging of popliteal lymph nodes was performed as described previously (Victora et al., 2010). In brief, mice were anaesthetized with 100 mg ketamine, 15 mg xylazine, and 2.5 mg acepromazine per kg body weight and were kept anaesthetized by inhalation of 1.25% isoflurane in 100% oxygen. The hind legs of mice were shaved, and mice were restrained on a stage warmer at 37°C (BioTherm Micro S37; Biogenics). The lymph node was exposed through an incision made on the hind leg and held in position using a metal strap with a small opening through which the node was imaged. Images were acquired at the Rockefeller University Bio-Imaging Resource Center using an upright microscope (BX61 with 25× NA 1.05 Plan water-immersion objective; Olympus) fitted with a laser (Chameleon Vision II; Coherent) tuned to 910 nm. Fluorescent emission was detected using a pair of overlapping CFP (460–510) and GFP (495–540) filters, separated by a 505 dichroic mirror, and a third filter (575–630) for the dsRed signal. For three-dimensional time series, we acquired 40-μm-deep z stacks with 5-μm z resolution, with an x–y resolution of 320 × 320 pixels and 1 μm/pixel, and a time resolution of 40 s/frame. Images were acquired using FluoView F1000 software (Olympus).

Intravital image analysis. Intravital 4D datasets were analyzed using Volocity software version 5.0 (PerkinElmer). For the quantification of T cell–B cell contacts, all OT-II T cells were manually inspected for interactions with B1-8^{hi} B cells of either genotype. Only long-lasting (>10 min), motile interactions in which B cells were leading the path of displacement were scored as T–B conjugates. Images were processed for presentation using Photoshop CS4. Videos were processed for presentation using After Effects version 8.0 (Adobe).

Statistical analysis. Multiple group comparisons were performed by analysis of variance with Tukey's post test. Intravital imaging quantification was performed by Fisher's exact test. All analyses were performed using Prism version 5.0b (GraphPad Software).

Online supplemental material. Fig. S1 shows a comparison of NP-PE–binding naive B cells in WT and MD4 mice. Fig. S2 shows the kinetics of appearance of histologically detectable GCs and of expression of GC-associated markers. Fig. S3 shows the in vitro characterization of the NP-Eα reagent. Fig. S4 shows DEC205 expression by flow cytometry on naive and GC B cells. Fig. S5 shows antigen delivery to B cells via DEC205. Videos 1 and 2 show multiphoton intravital time series of T cell–B cell interactions in T–B border clusters after treatment with α-DEC205–CS or α-DEC205–OVA, respectively. Table S1 lists the antibodies used for flow cytometry staining. Online supplemental material is available at http://www.jem.org/cgi/content/full/jem.20102477/DC1.

This work was supported in part by National Institutes of Health (NIH) grants R01 AI072529 (to M.C. Nussenzweig and M.L. Dustin) and R01 AI055037

(to M.L. Dustin). T.A. Schwickert was supported by the Schering foundation. D.R. Fooksman was supported by NIH training grant CA009161-34. M.C. Nussenzweig is a Howard Hughes Medical Institute Investigator. Support for the Rockefeller University multiphoton microscope was granted by the Empire State Stem Cell Fund through New York State Department of Health (NYSDOH) contract #C023046. Opinions expressed in this paper are solely those of the authors and do not necessarily reflect those of the Empire State Stem Cell Fund, the NYSDOH, or the State of New York.

The authors have no financial conflicts of interest.

Submitted: 26 November 2010
Accepted: 5 April 2011

REFERENCES

Allen, C.D., T. Okada, H.L. Tang, and J.G. Cyster. 2007. Imaging of germinal center selection events during affinity maturation. *Science*. 315:528–531. doi:10.1126/science.1136736

Allen, D., T. Simon, F. Sablitzky, K. Rajewsky, and A. Cumano. 1988. Antibody engineering for the analysis of affinity maturation of an anti-hapten response. *EMBO J.* 7:1995–2001.

Barnden, M.J., J. Allison, W.R. Heath, and F.R. Carbone. 1998. Defective TCR expression in transgenic mice constructed using cDNA-based alpha- and beta-chain genes under the control of heterologous regulatory elements. *Immunol. Cell Biol.* 76:34–40. doi:10.1046/j.1440-1711.1998.00709.x

Bonifaz, L., D. Bonnyay, K. Mahnke, M. Rivera, M.C. Nussenzweig, and R.M. Steinman. 2002. Efficient targeting of protein antigen to the dendritic cell receptor DEC-205 in the steady state leads to antigen presentation on major histocompatibility complex class I products and peripheral $CD8^+$ T cell tolerance. *J. Exp. Med.* 196:1627–1638. doi:10.1084/jem.20021598

Boscardin, S.B., J.C. Hafalla, R.F. Masilamani, A.O. Kamphorst, H.A. Zebroski, U. Rai, A. Morrot, F. Zavala, R.M. Steinman, R.S. Nussenzweig, and M.C. Nussenzweig. 2006. Antigen targeting to dendritic cells elicits long-lived T cell help for antibody responses. *J. Exp. Med.* 203:599–606. doi:10.1084/jem.20051639

Carrasco, Y.R., and F.D. Batista. 2007. B cells acquire particulate antigen in a macrophage-rich area at the boundary between the follicle and the subcapsular sinus of the lymph node. *Immunity*. 27:160–171. doi:10.1016/j.immuni.2007.06.007

Coffey, F., B. Alabyev, and T. Manser. 2009. Initial clonal expansion of germinal center B cells takes place at the perimeter of follicles. *Immunity*. 30:599–609. doi:10.1016/j.immuni.2009.01.011

Dal Porto, J.M., A.M. Haberman, G. Kelsoe, and M.J. Shlomchik. 2002. Very low affinity B cells form germinal centers, become memory B cells, and participate in secondary immune responses when higher affinity competition is reduced. *J. Exp. Med.* 195:1215–1221. doi:10.1084/jem.20011550

Draghi, N.A., and L.K. Denzin. 2010. H2-O, a MHC class II-like protein, sets a threshold for B-cell entry into germinal centers. *Proc. Natl. Acad. Sci. USA*. 107:16607–16612. doi:10.1073/pnas.1004664107

Ekiert, D.C., G. Bhabha, M.A. Elsliger, R.H. Friesen, M. Jongeneelen, M. Throsby, J. Goudsmit, and I.A. Wilson. 2009. Antibody recognition of a highly conserved influenza virus epitope. *Science*. 324:246–251. doi:10.1126/science.1171491

Fooksman, D.R., S. Vardhana, G. Vasiliver-Shamis, J. Liese, D.A. Blair, J. Waite, C. Sacristán, G.D. Victora, A. Zanin-Zhorov, and M.L. Dustin. 2010. Functional anatomy of T cell activation and synapse formation. *Annu. Rev. Immunol.* 28:79–105. doi:10.1146/annurev-immunol-030409-101308

Garside, P., E. Ingulli, R.R. Merica, J.G. Johnson, R.J. Noelle, and M.K. Jenkins. 1998. Visualization of specific B and T lymphocyte interactions in the lymph node. *Science*. 281:96–99. doi:10.1126/science.281.5373.96

Gonzalez, S.F., V. Lukacs-Kornek, M.P. Kuligowski, L.A. Pitcher, S.E. Degn, Y.A. Kim, M.J. Cloninger, L. Martinez-Pomares, S. Gordon, S.J. Turley, and M.C. Carroll. 2010. Capture of influenza by medullary dendritic cells via SIGN-R1 is essential for humoral immunity in draining lymph nodes. *Nat. Immunol.* 11:427–434. doi:10.1038/ni.1856

Goodnow, C.C., J. Crosbie, S. Adelstein, T.B. Lavoie, S.J. Smith-Gill, R.A. Brink, H. Pritchard-Briscoe, J.S. Wotherspoon, R.H. Loblay, K. Raphael, et al. 1988. Altered immunoglobulin expression and functional silencing of self-reactive B lymphocytes in transgenic mice. *Nature*. 334:676–682. doi:10.1038/334676a0

Guo, M., S. Gong, S. Maric, Z. Misulovin, M. Pack, K. Mahnke, M.C. Nussenzweig, and R.M. Steinman. 2000. A monoclonal antibody to the DEC-205 endocytosis receptor on human dendritic cells. *Hum. Immunol.* 61:729–738. doi:10.1016/S0198-8859(00)00144-0

Hadjantonakis, A.K., S. Macmaster, and A. Nagy. 2002. Embryonic stem cells and mice expressing different GFP variants for multiple non-invasive reporter usage within a single animal. *BMC Biotechnol.* 2:11. doi:10.1186/1472-6750-2-11

Jacob, J., R. Kassir, and G. Kelsoe. 1991. In situ studies of the primary immune response to (4-hydroxy-3-nitrophenyl)acetyl. I. The architecture and dynamics of responding cell populations. *J. Exp. Med.* 173:1165–1175. doi:10.1084/jem.173.5.1165

Jiang, W., W.J. Swiggard, C. Heufler, M. Peng, A. Mirza, R.M. Steinman, and M.C. Nussenzweig. 1995. The receptor DEC-205 expressed by dendritic cells and thymic epithelial cells is involved in antigen processing. *Nature*. 375:151–155. doi:10.1038/375151a0

Junt, T., E.A. Moseman, M. Iannacone, S. Massberg, P.A. Lang, M. Boes, K. Fink, S.E. Henrickson, D.M. Shayakhmetov, N.C. Di Paolo, et al. 2007. Subcapsular sinus macrophages in lymph nodes clear lymph-borne viruses and present them to antiviral B cells. *Nature*. 450:110–114. doi:10.1038/nature06287

Kamphorst, A.O., P. Guermonprez, D. Dudziak, and M.C. Nussenzweig. 2010. Route of antigen uptake differentially impacts presentation by dendritic cells and activated monocytes. *J. Immunol.* 185:3426–3435. doi:10.4049/jimmunol.1001205

Kim, H.J., B. Verbinnen, X. Tang, L. Lu, and H. Cantor. 2010. Inhibition of follicular T-helper cells by CD8(+) regulatory T cells is essential for self tolerance. *Nature*. 467:328–332. doi:10.1038/nature09370

King, C., S.G. Tangye, and C.R. Mackay. 2008. T follicular helper (TFH) cells in normal and dysregulated immune responses. *Annu. Rev. Immunol.* 26:741–766. doi:10.1146/annurev.immunol.26.021607.090344

Kroese, F.G., A.S. Wubbena, H.G. Seijen, and P. Nieuwenhuis. 1987. Germinal centers develop oligoclonally. *Eur. J. Immunol.* 17:1069–1072. doi:10.1002/eji.1830170726

Lindquist, R.L., G. Shakhar, D. Dudziak, H. Wardemann, T. Eisenreich, M.L. Dustin, and M.C. Nussenzweig. 2004. Visualizing dendritic cell networks in vivo. *Nat. Immunol.* 5:1243–1250. doi:10.1038/ni1139

Liu, Y.J., J. Zhang, P.J. Lane, E.Y. Chan, and I.C. MacLennan. 1991. Sites of specific B cell activation in primary and secondary responses to T cell-dependent and T cell-independent antigens. *Eur. J. Immunol.* 21:2951–2962. doi:10.1002/eji.1830211209

MacLennan, I.C. 1994. Germinal centers. *Annu. Rev. Immunol.* 12:117–139. doi:10.1146/annurev.iy.12.040194.001001

Mouquet, H., J.F. Scheid, M.J. Zoller, M. Krogsgaard, R.G. Ott, S. Shukair, M.N. Artyomov, J. Pietzsch, M. Connors, F. Pereyra, et al. 2010. Polyreactivity increases the apparent affinity of anti-HIV antibodies by heteroligation. *Nature*. 467:591–595. doi:10.1038/nature09385

Muramatsu, M., K. Kinoshita, S. Fagarasan, S. Yamada, Y. Shinkai, and T. Honjo. 2000. Class switch recombination and hypermutation require activation-induced cytidine deaminase (AID), a potential RNA editing enzyme. *Cell*. 102:553–563. doi:10.1016/S0092-8674(00)00078-7

Okada, T., M.J. Miller, I. Parker, M.F. Krummel, M. Neighbors, S.B. Hartley, A. O'Garra, M.D. Cahalan, and J.G. Cyster. 2005. Antigen-engaged B cells undergo chemotaxis toward the T zone and form motile conjugates with helper T cells. *PLoS Biol.* 3:e150. doi:10.1371/journal.pbio.0030150

Pape, K.A., D.M. Catron, A.A. Itano, and M.K. Jenkins. 2007. The humoral immune response is initiated in lymph nodes by B cells that acquire soluble antigen directly in the follicles. *Immunity*. 26:491–502. doi:10.1016/j.immuni.2007.02.011

Pasqualucci, L., A. Migliazza, N. Fracchiolla, C. William, A. Neri, L. Baldini, R.S. Chaganti, U. Klein, R. Küppers, K. Rajewsky, and R. Dalla-Favera. 1998. BCL-6 mutations in normal germinal center B cells: evidence of somatic hypermutation acting outside Ig loci. *Proc. Natl. Acad. Sci. USA*. 95:11816–11821. doi:10.1073/pnas.95.20.11816

Paus, D., T.G. Phan, T.D. Chan, S. Gardam, A. Basten, and R. Brink. 2006. Antigen recognition strength regulates the choice between extrafollicular plasma cell and germinal center B cell differentiation. *J. Exp. Med.* 203:1081–1091. doi:10.1084/jem.20060087

Pereira, J.P., L.M. Kelly, and J.G. Cyster. 2010. Finding the right niche: B-cell migration in the early phases of T-dependent antibody responses. *Int. Immunol.* 22:413–419. doi:10.1093/intimm/dxq047

Phan, T.G., I. Grigorova, T. Okada, and J.G. Cyster. 2007. Subcapsular encounter and complement-dependent transport of immune complexes by lymph node B cells. *Nat. Immunol.* 8:992–1000. doi:10.1038/ni1494

Qi, H., J.G. Egen, A.Y. Huang, and R.N. Germain. 2006. Extrafollicular activation of lymph node B cells by antigen-bearing dendritic cells. *Science.* 312:1672–1676. doi:10.1126/science.1125703

Qi, H., J.L. Cannons, F. Klauschen, P.L. Schwartzberg, and R.N. Germain. 2008. SAP-controlled T-B cell interactions underlie germinal centre formation. *Nature.* 455:764–769. doi:10.1038/nature07345

Rajewsky, K. 1996. Clonal selection and learning in the antibody system. *Nature.* 381:751–758. doi:10.1038/381751a0

Reif, K., E.H. Ekland, L. Ohl, H. Nakano, M. Lipp, R. Förster, and J.G. Cyster. 2002. Balanced responsiveness to chemoattractants from adjacent zones determines B-cell position. *Nature.* 416:94–99. doi:10.1038/416094a

Robbiani, D.F., A. Bothmer, E. Callen, B. Reina-San-Martin, Y. Dorsett, S. Difilippantonio, D.J. Bolland, H.T. Chen, A.E. Corcoran, A. Nussenzweig, and M.C. Nussenzweig. 2008. AID is required for the chromosomal breaks in c-myc that lead to c-myc/IgH translocations. *Cell.* 135:1028–1038. doi:10.1016/j.cell.2008.09.062

Robbiani, D.F., S. Bunting, N. Feldhahn, A. Bothmer, J. Camps, S. Deroubaix, K.M. McBride, I.A. Klein, G. Stone, T.R. Eisenreich, et al. 2009. AID produces DNA double-strand breaks in non-Ig genes and mature B cell lymphomas with reciprocal chromosome translocations. *Mol. Cell.* 36:631–641. doi:10.1016/j.molcel.2009.11.007

Rudensky, A.Yu., S. Rath, P. Preston-Hurlburt, D.B. Murphy, and C.A. Janeway Jr. 1991. On the complexity of self. *Nature.* 353:660–662. doi:10.1038/353660a0

Schaefer, B.C., M.L. Schaefer, J.W. Kappler, P. Marrack, and R.M. Kedl. 2001. Observation of antigen-dependent CD8+ T-cell/ dendritic cell interactions in vivo. *Cell. Immunol.* 214:110–122. doi:10.1006/cimm.2001.1895

Scheid, J.F., H. Mouquet, N. Feldhahn, M.S. Seaman, K. Velinzon, J. Pietzsch, R.G. Ott, R.M. Anthony, H. Zebroski, A. Hurley, et al. 2009. Broad diversity of neutralizing antibodies isolated from memory B cells in HIV-infected individuals. *Nature.* 458:636–640. doi:10.1038/nature07930

Schwickert, T.A., R.L. Lindquist, G. Shakhar, G. Livshits, D. Skokos, M.H. Kosco-Vilbois, M.L. Dustin, and M.C. Nussenzweig. 2007. In vivo imaging of germinal centres reveals a dynamic open structure. *Nature.* 446:83–87. doi:10.1038/nature05573

Schwickert, T.A., B. Alabyev, T. Manser, and M.C. Nussenzweig. 2009. Germinal center reutilization by newly activated B cells. *J. Exp. Med.* 206:2907–2914. doi:10.1084/jem.20091225

Shen, H.M., A. Peters, B. Baron, X. Zhu, and U. Storb. 1998. Mutation of BCL-6 gene in normal B cells by the process of somatic hypermutation of Ig genes. *Science.* 280:1750–1752. doi:10.1126/science.280.5370.1750

Shih, T.A., E. Meffre, M. Roederer, and M.C. Nussenzweig. 2002a. Role of BCR affinity in T cell-dependent antibody responses in vivo. *Nat. Immunol.* 3:570–575. doi:10.1038/ni803

Shih, T.A., M. Roederer, and M.C. Nussenzweig. 2002b. Role of antigen receptor affinity in T cell-independent antibody responses in vivo. *Nat. Immunol.* 3:399–406. doi:10.1038/ni776

Suzuki, K., I. Grigorova, T.G. Phan, L.M. Kelly, and J.G. Cyster. 2009. Visualizing B cell capture of cognate antigen from follicular dendritic cells. *J. Exp. Med.* 206:1485–1493. doi:10.1084/jem.20090209

Victora, G.D., T.A. Schwickert, D.R. Fooksman, A.O. Kamphorst, M. Meyer-Hermann, M.L. Dustin, and M.C. Nussenzweig. 2010. Germinal center dynamics revealed by multiphoton microscopy with a photoactivatable fluorescent reporter. *Cell.* 143:592–605. doi:10.1016/j.cell.2010.10.032

Vintersten, K., C. Monetti, M. Gertsenstein, P. Zhang, L. Laszlo, S. Biechele, and A. Nagy. 2004. Mouse in red: red fluorescent protein expression in mouse ES cells, embryos, and adult animals. *Genesis.* 40:241–246. doi:10.1002/gene.20095

Vinuesa, C.G., M.C. Cook, C. Angelucci, V. Athanasopoulos, L. Rui, K.M. Hill, D. Yu, H. Domaschenz, B. Whittle, T. Lambe, et al. 2005. A RING-type ubiquitin ligase family member required to repress follicular helper T cells and autoimmunity. *Nature.* 435:452–458. doi:10.1038/nature03555

SUPPLEMENTAL MATERIAL

Schwickert et al., http://www.jem.org/cgi/content/full/jem.20102477/DC1

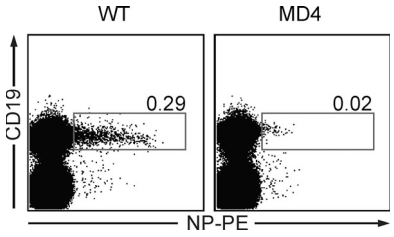

Figure S1. Low level of NP–PE binding in MD4 mice. Flow cytometric analysis of NP-PE binding to WT and MD4 B cells. Mice were injected into the footpads and base of tail with a total of 50 µg NP-PE, and draining lymph nodes were extracted 16 h later for flow cytometry analysis. Data are representative of two independent experiments with one to two mice per condition per experiment.

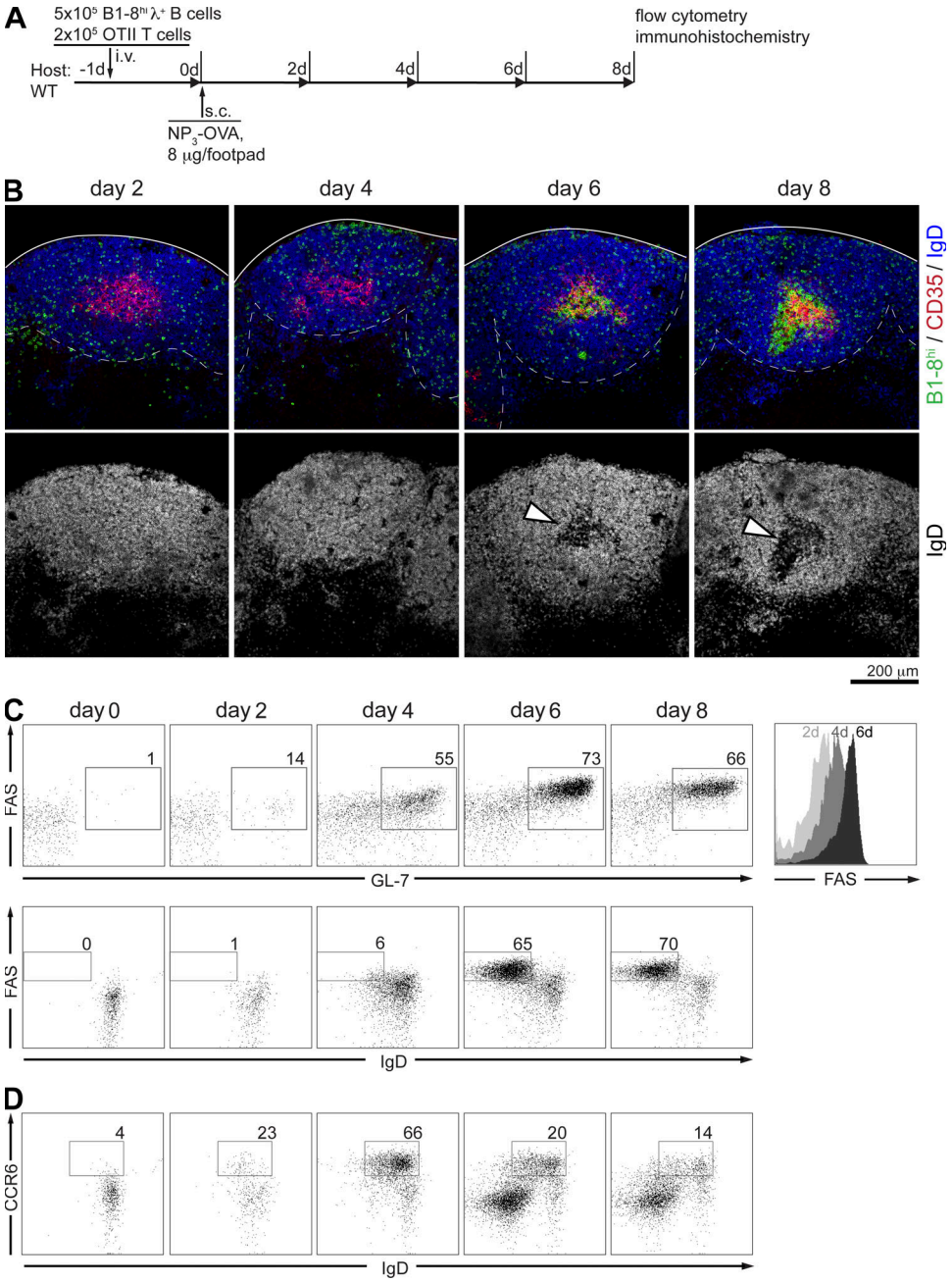

Figure S2. Kinetics of GC formation. (A) Diagrammatic representation of the experimental protocol. (B) Histology of B cell follicles in draining lymph nodes at day 0, 2, 4, 6, and 8 after immunization. (top) Representative images of B1-8^{hi}CFP^{+} B cells (green) in B cell follicles, identified by CD35 (red) and IgD (blue) staining. The dashed line indicates the border between the B cell follicle and T cell zone. (bottom) GCs can by identified by the absence of IgD^{+} B cells, indicated by arrowheads. (C) Flow cytometry of transferred B1-8^{hi} B cells. (top) FAS/GL-7 expression. (bottom) FAS/IgD expression. (D) Flow cytometry of transferred B1-8^{hi} B cells; CCR6/IgD expression. All data are representative of at least two independent experiments.

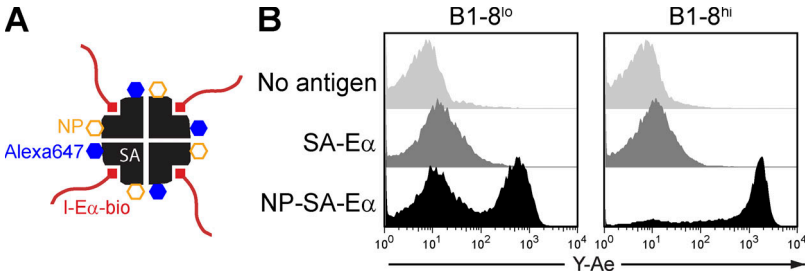

Figure S3. Measuring BCR-mediated antigen presentation using NP-Eα. (A) Cartoon representing the NP-Eα reagent. (B) Flow cytometry plot showing antigen presentation (binding of Y-Ae anti-pMHC antibody) by purified splenic B cells cultured in vitro for 16 h with 1 µg/ml NP-SA-Eα or control SA-Eα reagents. Gated on live CD19^{+}Igκ^{-} cells. Data are representative of three experiments.

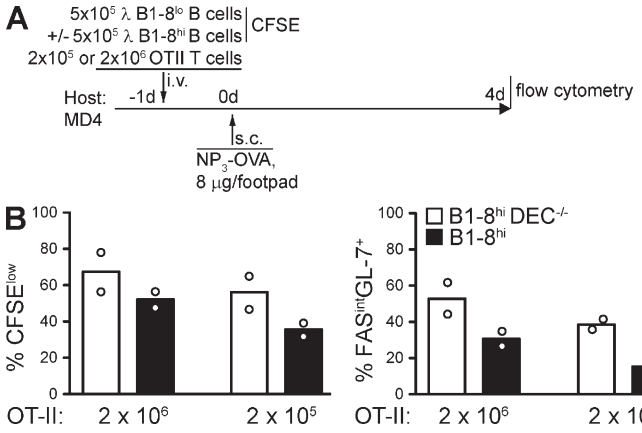

Figure S4. Effect of the number of T cell precursors on pre-GC competition. (A) Diagrammatic representation of the experimental layout. (B) Flow cytometric analysis of proliferation (CFSE dilution) and activation (expression of GL-7 and FAS) among transferred B1-8^{hi}CFP^{+} and B1-8^{lo}CD45.1^{+} CFSE-labeled B cells in draining lymph nodes 4 d after immunization. The number of T cells transferred is indicated below the chart. Each symbol represents one mouse. Data are from one experiment with two mice per condition.

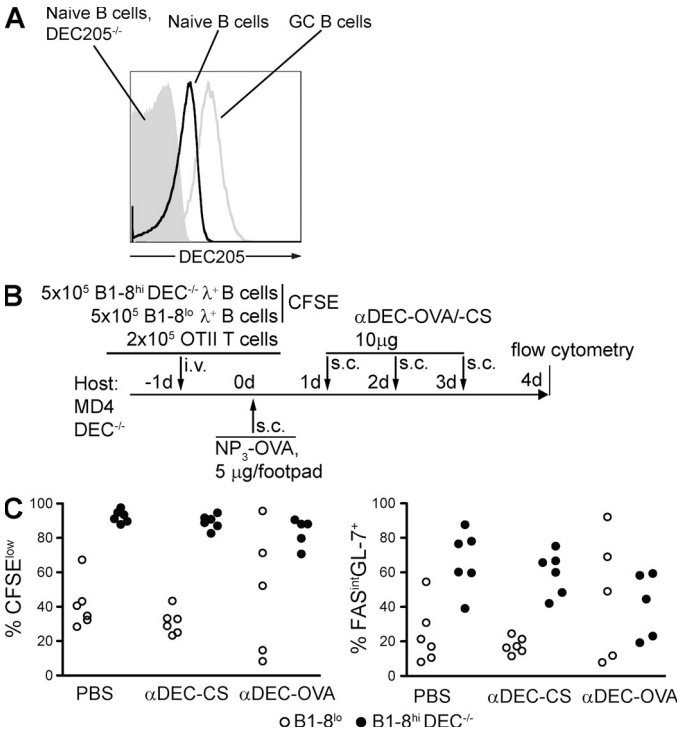

Figure S5. Antigen delivery to B cells via DEC205. (A) Flow cytometric analysis of DEC205 expression on naive and GC B cells. DEC205$^{-/-}$ B cells are shown as a negative control. Data are representative of multiple experiments. (B) Diagrammatic representation of the experimental protocol in C. (C) Flow cytometric analysis of proliferation (CFSE dilution) and activation (expression of GL-7 and FAS) among transferred B1-8^{lo}DEC205$^{+/+}$CFP^{+} and B1-8^{hi}DEC205$^{-/-}$CD45.1^{+} CFSE-labeled B cells in draining lymph nodes 4 d after immunization. Each symbol represents one mouse. Data are from three independent experiments with one to two mice per condition per experiment.

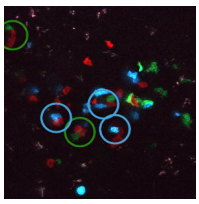

Video 1. T cell–B cell contacts in mice treated with anti-DEC205–CS. Red indicates OT-II T cells, green indicates B1-8^{hi} B cells, and cyan indicates B-18^{hi}DEC205$^{-/-}$ B cells. Long-lasting (>10 min) motile conjugates are marked by circles colored according to B cell genotype. This video is shown at 7 frames/s.

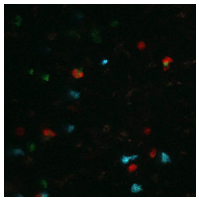

Video 2. T cell–B cell contacts in mice treated with anti-DEC205–OVA. Red indicates OT-II T cells, green indicates B1-8^{hi} B cells, and cyan indicates B-18^{hi}DEC205$^{-/-}$ B cells. Long-lasting (>10 min) motile conjugates are marked by circles colored according to B cell genotype. This video is shown at 7 frames/s.

Table S1. List of antibodies used for flow cytometry

Surface molecule	Fluorochrome	Clone	Manufacturer	Final concentration
				μg/ml
220	PerCP	RA3-6B2	BD	1.0
CR6	PE	29-2L17	BioLegend	4.0
D19	APC-Cy7	1D3	BD	2.0
CD45	PE	30-F11	eBioscience	1.0
D45.1	APC	A20	BD	1.0
CD45.1	APC-eFluor780	A20	eBioscience	1.0
CD45.2	PE	104	BD	1.0
CD45.2	PerCP-Cy5.5	104	eBioscience	0.5
CD138	PE	281-2	BD	1.0
DEC205	APC	205yekta	eBioscience	0.2
FAS	PE-Cy7	Jo2	BD	0.25
GL-7	Biotin	GL-7	BD	1.0
GL-7	FITC	GL-7	BD	1.0
GL-7	Alexa Fluor 647	GL-7	eBioscience	0.5
$I\text{-}A^b$ ($I\text{-}E\alpha_{52-68}$)	Biotin	Y-Ae	eBioscience	2.5
IgD	Alexa Fluor 647	11-26	eBioscience	2.5
IgG_1	APC	X56	BD	1.0
Igκ	PE	187.1	BD	0.067
$Ig\lambda_{1-3}$	Conjugated to Alexa Fluor 700	R26-46	BD	0.625
SA	PerCP	NA	BD	0.67
SA	PE	NA	BD	0.5

NA, not applicable.